

PCCP

Accepted Manuscript



This is an *Accepted Manuscript*, which has been through the Royal Society of Chemistry peer review process and has been accepted for publication.

Accepted Manuscripts are published online shortly after acceptance, before technical editing, formatting and proof reading. Using this free service, authors can make their results available to the community, in citable form, before we publish the edited article. We will replace this *Accepted Manuscript* with the edited and formatted *Advance Article* as soon as it is available.

You can find more information about *Accepted Manuscripts* in the [Information for Authors](#).

Please note that technical editing may introduce minor changes to the text and/or graphics, which may alter content. The journal's standard [Terms & Conditions](#) and the [Ethical guidelines](#) still apply. In no event shall the Royal Society of Chemistry be held responsible for any errors or omissions in this *Accepted Manuscript* or any consequences arising from the use of any information it contains.

Dynamic Spreading of a Nanosized Droplet on a Solid in an Electric Field

Cite this: DOI: 10.1039/x0xx00000x

F. H. Song^a, B. Q. Li^{b,*}, Y. Li^a

Received 00th October 2014,

Accepted 00th January 2014

DOI: 10.1039/x0xx00000x

www.rsc.org/

Molecular dynamic simulations are performed for the dynamic spreading of a nanosized water droplet subject to a parallel electric field. Results show the droplet spreads asymmetrically in a weak field but symmetrically in a strong field. The initial conditions affect the dynamic spreading behavior but not the final equilibrium shapes.

Wetting phenomena are ubiquitous and essential in a variety of natural and technological processes. And the microscopic mechanism of solid-liquid contact is characterized by the liquid-solid contact angle¹⁻⁵. ~~Equilibrium contact angle is insensitive to external fields within some assumptions on the nature of these fields⁵.~~ Currently, the electrowetting behavior of ionic liquids has attracted a great deal of attentions, because electrowetting is widely used to manipulate tiny amounts of liquids on surfaces⁶⁻⁹. It has found applications ranging from microelectronic cooling to miniaturized on-chip biosensing⁹. In electrowetting, the wetting behavior of a droplet on a planar solid surface is modified by an applied electric field. Bormashenko¹⁰ derived the well-known Young-Lippmann equation by imposing the transversality conditions on the appropriate variational problems of wetting when interfacial tension depends on electric field. The Young-Lippmann equation relates the change of the contact angle to the electric field¹¹.

$$\cos \theta = \frac{\gamma_{sg} - \gamma_{sl}}{\gamma_{lg}} + \frac{\langle \epsilon \epsilon_0 \mathbf{E} \mathbf{E} \rangle D}{2\gamma_{lg}} \quad (1)$$

where θ is the contact angle, D the thickness of the interfacial double layer, γ the surface tension, \mathbf{E} the applied electric field, ϵ the dielectric constant of the liquid and ϵ_0 the dielectric constant of free space. Also, the subscripts l , g and s refer to the liquid, gas and solid, respectively, and the angular bracket stands for the average over D . According to equation (1), the contact angle depends solely on the field strength.

Recently, molecular dynamic (MD) simulations show that the Young-Lippmann equation in general is not valid for a nanosized droplet electrically-spreading on a solid substrate¹¹.

¹². Perhaps, when it comes to nanosized droplet, the macroscopic notions, such as surface tension, contact angle are not applicable. For polar fluids like water, both the field strength and the field direction can have a strong effect on the equilibrium shape of the nanosized droplet. The interaction of the water molecules with the field, combined with the contributions from various intermolecular forces, can lead to novel nanoscaled phenomena unencountered in electrowetting of macrosized liquid droplets. For instance, under an electric field, a nanosized droplet may electrowet the solid either asymmetrically or symmetrically, depending on the field strength and directions. This may potentially open up new avenues to manipulate a nanosized droplet by the use of an external electric field. To date, studies on electrowetting of nanosized droplets on solids have been largely focused on the behavior of static liquid-solid contact, which is characterized by static contact angles. The dynamics of spontaneous electrowetting of a droplet has been studied experimentally for a macrosized droplet, whose static contact angle as affected by an electric field obeys the Young-Lippmann equation^{13,14}. The dynamics of a nanosized drop, as it spreads on a solid in an electric field, appears to have been elusive.

In this communication, the dynamics of the spreading of a nanosized droplet on a solid substrate under the influence of an electric field is studied using MD simulations. While spontaneous spreading has been studied for macroscopic droplets in an electric field, nanoscale droplets exhibit new phenomena unseen in macrodroplets, due to the small scales involved. For nanoscaled liquids, MD simulations offer a useful tool for analysis. In comparison with the dynamic spreading of a nanosized droplet on a solid in the absence of an external field^{15,16}, some novel features of dynamic spreading as affected by an electric field arise as a result of the molecular interactions with the field.

In MD simulations, the solid substrate assumes a diamond-like structure and the water molecule assumes a simple point charge/extension (SPC/E)¹⁷. The solid substrate consists of

10,816 atoms arranged in diamond cubic lattice, with lattice constant of 5.4307 Å. The solid substrate is considered as rigid in order to speed up the computer simulations^{11,12,18}. The molecule (SPC/E model) takes a tetrahedral shape with two hydrogen atoms connecting to the oxygen atom through covalent bonds. Hydrogen is positively charged, while oxygen negatively. The intermolecular interactions are calculated as follows. The electrostatic interaction is modeled using Coulomb's law, while the dispersion and repulsion force using the Lennard-Jones (L-J) potential^{17,18}.

$$\phi(r_{ij}) = 4\epsilon_{oo} \left[\left(\frac{\sigma_{oo}}{r_{oo}} \right)^{12} - \left(\frac{\sigma_{oo}}{r_{oo}} \right)^6 \right] + \frac{1}{4\pi\epsilon_0} \sum_{i=1}^3 \sum_{j=1}^3 \frac{q_i q_j}{r_{ij}} \quad (2)$$

where the first term L-J potential is applied only for oxygen-oxygen interaction, with $\sigma_{oo} = 3.166$ Å and $\epsilon_{oo} = 0.1556$ Kcal/mole. The last term in Eq. (2) describes the Coulomb force between the charged atoms, where q_i is the charge on atom i , r_{ij} is the distance between atoms i and j , and ϵ_0 is the dielectric constant for vacuum. In our studies, it is normalized as 1.

The interaction between the water and solid substrate is also modeled by the modified L-J potential¹⁹. With an electric field E present, the electric force $f_{ie} = q_i E$ is exerted on each atom according to its charge q_i , which is treated in the MD simulations as discussed in²⁰. For the results presented below, a nanosized droplet of 2,000 water molecules was used, as suggested in reference²¹. The electrowetting calculations start with a droplet of perfect sphericity, which is obtained through a separate MD simulation with gravity neglected. The Nose-Hoover thermostat²² was used at every time step to make sure that the ensemble is kept at a desired temperature 300K, which can take the energy created by the exerted electric fields in simulations. Other MD simulation details, such as periodic boundaries, are standard and thus be omitted. Unless otherwise indicated, the electric field is applied in parallel to the solid surface (in the x -direction) before the liquid droplet attaches the solid. Under electric field, the dynamic contact angle is obtained as the average value for 10 snapshots extracted every 50 time steps around a time point.

Besides, one dimensionless constant ξ , describing the interrelation of electric field and surface tension effect could be introduced as²³,

$$\xi = \frac{\epsilon_0 \epsilon E^2 V}{2\gamma S} \quad (3)$$

where V and S are the volume and surface of the droplet respectively. For the water droplet in the present paper, V/S is assumed to be about $1/3R$, surface tension $\gamma = 71$ mJ/m², dielectric constant $\epsilon = 79$, the vacuum dielectric constant $\epsilon_0 = 8.85 \times 10^{-12}$ F/m.²⁴

Firstly, when electric field is free, the equilibrium contact angle of water droplet on silicon solid substrate is measured to check our simulation model. It was 86.4 degree, which is well consistent with experimental data reported in literatures^{25,26}.

The applied electric field strengths warrant explanation. In the paper, electric field of 0.1 and 0.5V/Å were applied to study the dynamic spreading process of water droplet on a solid substrate. The actual strength of electric field differs significantly from the unperturbed applied field. The actual electric field \bar{E} is lowered by orientational polarization of water molecules. For example, when the normal input electric field strength is 0.2 V/Å, the corresponding average actual field \bar{E} equals to 0.005V/Å in equilibrium with a field-free aqueous reservoir²⁷. These actual fields \bar{E} applied here are too weak to

polarize significantly. Water molecules cannot be decomposed under this strength of electric field.

In Figure 1, the dynamic spreading of a nanodroplet on a solid, as illustrated by several time-snapshots, is contrasted for two different electric field strengths applied. Here the x -coordinate points from the left to right. Clearly, the droplet electrowets the solid rather differently for these two cases and the electric field strength has a strong effect on both the final equilibrium states and the dynamics of the spreading. For a weak field (0.05 V/Å), the droplet dynamically spreads asymmetrically along the field direction. For the trailing surface, that is, the surface of the droplet whose outward normal forms an acute angle with the field (or $x+$) direction, the electric field helps the droplet in wetting the solid. In this case, the leading angle, that is, the angle formed between the tangential of the surface contour line of the droplet and the solid on the x - y plane, reduces from obtuse to acute as the spreading evolves, exhibiting the electrowetting effect. For the leading surface, whose outward normal forms an obtuse angle with the field direction, the eventual electrowetting never occurs. The final equilibrium shape of the droplet is asymmetric with respect to the y - z plane. During the entire process of spreading, the droplet remains symmetric with respect to the x - y plane.

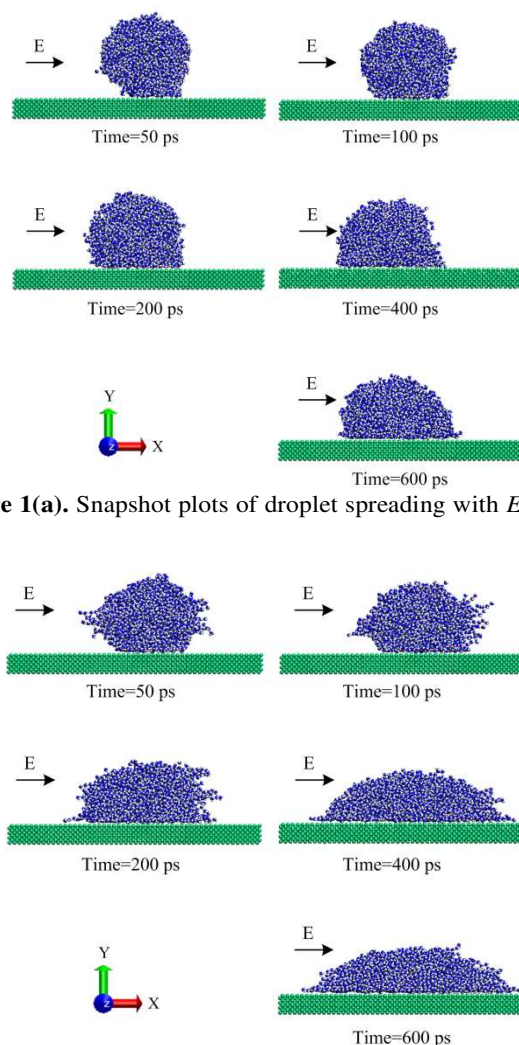


Figure 1(a). Snapshot plots of droplet spreading with $E_x = 0.05$ V/Å.

Figure 1(b). Snapshot plots of droplet spreading with $E_x = 0.1$ V/Å.

To further understand the dynamics of the droplet spreading, the evolution of the dynamic leading and trailing contact angles is shown in Figure 2. It is seen from Figure 2(a) that the asymmetry starts as soon as the liquid droplet starts to spread on the solid and difference between the leading and trailing contact angles continues to increase until the final equilibrium state in spreading is reached. For this particular case, the equilibrium reaches at $t=400$ ps.

Turning to the case of the strong field ($E_x = 0.1 \text{ V/\AA}$), we see from Figure 1(b) that the droplet spreads on the solid in a different manner than the case of $E_x = 0.05 \text{ V/\AA}$. The droplet remains symmetric with respect to both the x - y and y - z planes and the leading and trailing contact angles remain about the same. It eventually electrowets the surface. Figure 2(b) plots the evolution of the dynamic contact angles at the leading and trailing positions, which confirms that the symmetric spreading behavior of the droplet with a stronger field.

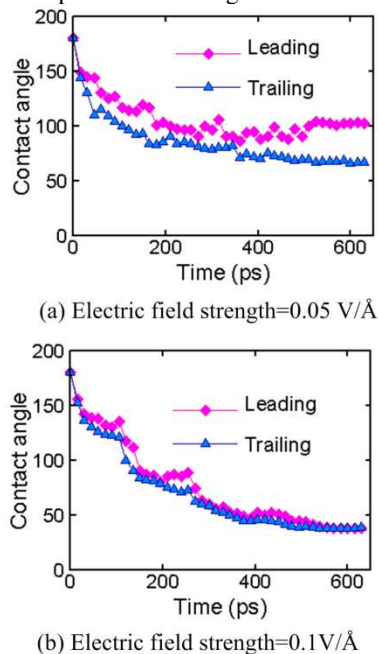


Figure 2. Dynamic contact angles (leading and trailing) for (a) $E_x = 0.05 \text{ V/\AA}$ and (b) $E_x = 0.1 \text{ V/\AA}$, diamond represents leading contact angle and triangle represents trailing contact angle.

MD simulations also have been conducted of the droplet spreading with its equilibrium shape on the solid without an electric field to investigate the effect of the initial conditions. It is found that the initial conditions do not affect the final equilibrium shapes but do affect the dynamic behavior during spreading. Figure 3 plots the evolution of the dynamic leading and trailing angles of the nanodroplet as it spreads on solid with $E_x = 0.1 \text{ V/\AA}$. Comparison of Figure 2(a) and Figure 3 indicates that when the droplet starts with its equilibrium spreading condition without E field, the dynamics entails a different leading wetting process than the trailing, as the droplet spreads on the solid with $E_x = 0.1 \text{ V/\AA}$, until almost the point when the final equilibrium is reached. During the initial stage of dynamic spreading, the leading angle experiences an increase before joining the trailing angle eventually (see Figure 3).

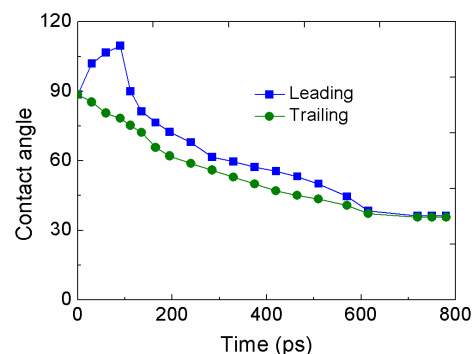


Figure 3. Dynamic contact angles (leading and trailing) for $E_x = 0.1 \text{ V/\AA}$ applied after the free droplet on solid surface reached to the equilibrium state, square represents leading contact angle and circle represents trailing contact angle.

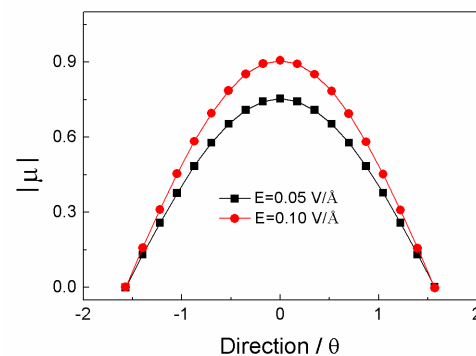


Figure 4. Distribution of the water molecular dipole moment vector near the liquid-solid interface in the presence of electric fields: $E_x = 0.05$ and 0.1 V/\AA .

The physical mechanisms for the dynamic spreading of the nanodroplet on solid with an E field can be rather complex. The interaction of the electric field with the polar water molecules, the intermolecular forces and the hydrogen bonds all contribute to the droplet deformation process. Detailed analysis of MD simulations reveals that the surface tension is related to the number of hydrogen bonds on the surface of a water droplet. To be specific, a bigger number of hydrogen bond leads to a weaker surface tension^{6, 24, 28}. A water molecule consists of one heavy oxygen atom and two light hydrogen atoms. The oxygen atom is electronegative and the hydrogen electropositive, forming an electric point dipole. In water, hydrogen bonds exist to network the entire water droplet. The oxygen of a polar water molecule has two lone pairs of electrons, each of which allows a hydrogen bond to be formed with a hydrogen atom on another water molecule. Every water molecule is hydrogen-bonded with up to four other molecules in its neighborhood, two being through its two lone pairs, and the other two through its two hydrogen atoms.

With an applied electric field, the electric force realigns the polar water molecular dipole such that the heavy oxygen atom moves against the field and the light hydrogen atom along the field direction. This realignment causes the oxygen atoms to collect on the leading surface and the hydrogen atoms on the trailing surface. During the realignment process, the hydrogen bonds are broken or generated, with a net reduction in hydrogen bonds to cause the droplet to spread. Calculated from the simulation data, the distribution of dipole moment vector μ as a

function of the angles between dipole vector and solid surface was shown in Figure 4. As it is expected, the distributions of μ peak at dipole orientations parallel to the interface. For a weak electric field ($E=0.05 \text{ V/\AA}$), the dimensionless constant ξ calculated from equation 3 is 1.0, indicating that the electric field and surface tension have the same induced effects on the spreading process. The water molecule realigns itself only partially. Consequently, more hydrogen bonds associated with the oxygen atom are broken than those associated with the hydrogen. This imbalance on hydrogen bonds between the leading and trailing surfaces leads to the asymmetric spreading of the nanodroplet on solid in response to a weak electric field. For a stronger electric field ($E=0.1 \text{ V/\AA}$), the dimensionless constant ξ calculated from equation 3 is 4.1. The electric field plays a more decisive role on the spreading. The polar molecules re-align themselves almost completely with the molecular dipole point to the same direction as the electric field. This results in a balanced net reduction in hydrogen bonds on both the leading and trailing surfaces of the droplet, and as a consequence the droplet spreads symmetrically on the solid. This is consistent with the results on hydrogen bond data obtained from simulations in the present study. For example, at $E=0.05 \text{ V/\AA}$, the mean hydrogen bond numbers in the interface near the leading and the trailing edges of the droplet are 2.826 and 2.708 respectively. This suggests a smaller γ_{lg} and thus a larger leading contact angle, since $\gamma_{sl} - \gamma_{sg}$ is affected equally at both sides^{11,27}. In contrast, at $E=0.1 \text{ V/\AA}$, the mean hydrogen bond numbers in the interface near the leading and the trailing edges of the droplet are 2.643 and 2.641, which clearly suggest a symmetric spreading, that is, the leading and trailing contact angles being the same.

Conclusions

This paper has presented an MD study of the dynamical spreading of a nanosized water droplet on a solid substrate in an electric field. Polar water molecules interact with the applied electric field and re-orient their point dipoles, which determine the spreading behaviors. The applied electric field strength has a strong effect on both the final equilibrium states and the dynamics of the spreading. For a weaker field of 0.05 V/\AA , the droplet spreads asymmetrically with the leading contact angle being greater than the trailing contact angle. While for a stronger field of 0.1 V/\AA , in the dynamic spreading process, the droplet remains symmetric with respect to both the x-y and y-z planes and the leading and trailing contact angles remain about the same. Case studies indicate that the initial conditions do not affect the final equilibrium shapes but do affect the dynamical behavior of the droplet during spreading. The dynamics of the droplet spreading is controlled by a competing mechanism among the electric field force, water-water, and water-solid intermolecular forces.

Notes and references

^a School of Energy and Power Engineering, Northeast Dianli University, Jilin, 132012, China

^b Department of Mechanical Engineering, University of Michigan, Dearborn, MI 48128, USA

* Email: benqli@umich.edu; Tel: (+1)313-593-5241; Fax: (+1)313-593-3851

- H. K. Guo and H. P. Fang, *Chinese Phys. Lett.* 2005, **22**, 787-790.
- A. P. Malanoski, B. J. Johnson and J. S. Erickson, *Nanoscale*, 2014, **6**, 5260.
- G. Whyman, E. Bormashenko and T. Stein, *Chem. Phys. Lett.* 2008, **450**, 355-359.
- A. Deák, E. Hild, A. L. Kovács and Z. Hórvölgyi, *Phys. Chem. Chem. Phys.*, 2007, **9**, 6359-6370.
- E. Bormashe, *Colloids and Surfaces A: Physicochem. Eng. Aspects*, 2009, **345**, 163-165.
- F. Mugele and J. C. Baret, *Phys.: Condens. Matter*. 2005, **17**, R705-R774.
- M. G. Pollack, A. D. Shenderov and R. B. Fair, *The Royal Society of Chemistry, Lab Chip*, 2002, **2**, 96-101.
- M. Washizu, *IEEE Transactions on Industry Applications*, 1998, **34**(4), 732-737.
- S. Cho, H. Moon and C. J. Kim, *J. Microelectromechanical Systems*, 2003, **12**(1), 70-80.
- E. Bormashenko, *Mathematical Modelling of Natural Phenomena*, 2012, **7**(04), 1-5.
- C. D. Daub, D. Bratko, K. Leung and A. Luzar, *J. Phys. Chem. C*. 2007, **111**(2), 505-509.
- T. Yen, *Mol. Simul.* 2011, **38**(6), 509-507.
- S. R. Mahmoudi, K. Adamiak and G. S. Peter Castle, *Proc. R. Soc. A*, 2011, **467**(2135), 3257-3271.
- C. Decamps and J. D. Coninck, *Langmuir*, 2000, **16**(26), 10150-10153.
- N. Sedighi, S. Murad and S. K. Aggarwal, *Fluid Dyn. Res.* 2011, **43**, 015507.
- N. Sedighi, S. Murad and S. K. Aggarwal, *Fluid Dyn. Res.* 2010, **42**, 035501.
- H. J. C. Berendsen, J. R. Grigera and T. P. Straatsma, *J. Phys. Chem.* 1987, **91**, 6269.
- B. J. Kirby, *Micro- and Nanoscale Fluid Mechanics: Transport in Microfluidic Devices*. 2010.
- M. P. Allen, D. J. Tildesley, *Computer Simulation of Liquids* (Oxford Oxford University Press). 1989.
- S. Park and K. Schulten, *J. Chem. Phys.* 2004, **120**(13), 5946.
- W. B. Streett, D. J. Tildesley and G. Saville, *Mol. Phys.*, 1978, **35**(3) 639-648.
- P. H. Hünenberger, *Advances in Polymer Science*, 2005, **173**, 105-149.
- E. Bormashenko, R. Pogreb, R. Balter, O. Gendelman and D. Aurbach, *Appl. Phys. Lett.* 2012, **100**, 151601.
- I. V. Stiofkin, C. Weeraman, P. A. Pieniazek, F. Y. Shalhout, J. L. Skinner and A. V. Benderskii, *Nature*, 2011, **474**, 192-195.
- B. Arkles, *Hydrophobicity, Paint Coat. Ind. Mag.* 2006, **22**, 114-132.
- B. S. Kim, S. Shin, S. J. Shin, K. M. Kim and H. H. Cho, *Nanoscale Research Letters*, 2011, **6**, 333.
- C. D. Daub, D. Bratko and A. Luzar, *Top. Curr. Chem.* 2012, **307**, 155-179.
- Z. Zhang, L. Piatkowski, H. J. Bakker and M. Bonn, *Nature (Chemistry)*, 2011, **3**, 888-893.